Muscle Cross-Bridges Bound to Actin Are Disordered in the Presence of 2,3-Butanedione Monoxime

Liang Zhao, Nariman Naber, and Roger Cooke
Department of Biochemistry and Biophysics and the Cardiovascular Research Institute, University of California, San Francisco, San Francisco, California 94143 USA

ABSTRACT Electron paramagnetic resonance spectroscopy was used to monitor the orientation of muscle cross-bridges attached to actin in a low force and high stiffness state that may occur before force generation in the actomyosin cycle of interactions. 2,3-butanedione monoxime (BDM) has been shown to act as an uncompetitive inhibitor of the myosin ATPase that stabilizes a myosin·ADP·P_i complex. Such a complex is thought to attach to actin at the beginning of the powerstroke. Addition of 25 mM BDM decreases tension by 90%, although stiffness remains high, 40–50% of control, showing that cross-bridges are attached to actin but generate little or no force. Active cross-bridge orientation was monitored via electron paramagnetic resonance spectroscopy of a maleimide spin probe rigidly attached to cys-707 (SH-1) on the myosin head. A new labeling procedure was used that showed improved specificity of labeling. In 25 mM BDM, the probes have an almost isotropic angular distribution, indicating that cross-bridges are highly disordered. We conclude that in the pre-powerstroke state stabilized by BDM, cross-bridges are attached to actin, generating little force, with a large portion of the catalytic domain of the myosin heads disordered.

INTRODUCTION

Muscle contraction results from a cyclic interaction between myosin heads (cross-bridges) and actin, coupled with MgATP hydrolysis. Studies of the interaction of purified proteins and of the mechanics of active fibers have suggested that a myosin·ADP·P_i complex initially attaches to actin in a low force, pre-powerstroke state. The release of P_i, or isomerizations that accompany it, allow the transition to a force-producing state (reviewed in Cooke, 1986; Goldman, 1987). The atomic level structures of both actin and myosin have now been determined (Homes et al., 1990; Rayment et al., 1993a), and these structures have been used to define a low resolution structure of the actomyosin complex (Rayment et al., 1993b; Schroder et al., 1993). These results have led to a model for the changes in protein conformation that result in force generation (Rayment et al., 1993b). The structural data suggest that, before P_i release, myosin and actin are attached to each other via the electrostatic interaction of two opposing regions of their respective polypeptide chains. The region on myosin is highly disordered in the crystal structure, suggesting that in this interaction the myosin and actin are only weakly attached to one another. A tighter and more specific interaction between the two proteins is prevented by the conformation of the myosin head. The release of P_i then permits a deep cleft in the myosin structure to close, relieving the inhibition. This leads to a tighter bond with actin and to the working cross-bridge powerstroke. Understanding the structure of the actomyosin complex before the release of P_i will provide information on the events that occur within the powerstroke.

A number of approaches have been employed to define the structures of various complexes of myosin with actin. The rigor state is easily achieved by the elimination of substrate and is generally thought to represent that found at the end of the working powerstroke. The structures of other states in the active cycle, such as the pre-powerstroke state(s), have been more difficult to study, however, because of their transient nature. One approach to this problem has been to seek inhibitors that interact with, and stabilize, specific intermediate states of the ATPase cycle. One of these inhibitors is a small molecule, 2,3-butanedione monoxime (BDM), which has been shown to be an uncompetitive inhibitor of the actomyosin ATPase cycle. BDM reversibly suppresses the twitch and tetanic tension of both intact and skinned muscle (Fryer et al., 1988; Blanchard et al., 1990; Horiuti et al., 1988; Bagni et al., 1992; Belknap et al., 1993; Zhao and Kawai, 1994). BDM decreases the maximal contraction velocity and the isometric tension but increases the curvature of the force-velocity relation and the stiffness-to-tension ratio (Bagni et al., 1992). These investigators concluded that BDM reduces the attachment rate of cross-bridges to actin and lowers the force generation per cross-bridge. Biochemical studies indicate that BDM elevates the rate of the ATP hydrolysis step and stabilizes an intermediate state in the actomyosin cycle (Higuchi and Takemori, 1989; Herrmann et al., 1992). Together these studies have shown that BDM binds to and stabilizes states in which myosin is bound to the products of ATP hydrolysis, ADP and P_i, and that this myosin products complex can bind to actin. As noted, a similar complex is thought to be a transient intermediate that occurs before force production in the cycle. In the present work, we shall correlate solution biochemistry, fiber mechanics, and structural

Received for publication 18 April 1994 and in final form 27 January 1995.
Address reprint requests to Dr. Liang Zhao, Department of Biochemistry and Biophysics, Cardiovascular Research Institute, University of California, San Francisco, CA 94143. Tel.: 415-476-4836.

0006-3495/95/05/1980/11 $2.00

studies to better define the chemomechanics of weakly bound, pre-powerstroke states.

Spectroscopic probes provide one tool for investigating the orientation and mobility of specific sites on the contractile proteins in a muscle fiber. The use of paramagnetic probes to study cross-bridge energetics has several advantages over other biological techniques such as x-ray diffraction and electron microscopy (Barnett et al., 1986; Thomas, 1987). Previous studies have shown that one can selectively and rigidly label a reactive sulfhydryl (SH-1, cys-707) on the cross-bridge with paramagnetic probes and then use electron paramagnetic resonance (EPR) spectroscopy to monitor the orientation and rotation of the cross-bridge. Thomas and Cooke (1980) have shown that the probes attached to cys-707 are highly oriented when cross-bridges are tightly bound to actin in the absence of substrate (rigor) and are disordered when cross-bridges are detached from actin (relaxation). EPR spectra of active fibers can be interpreted as a linear combination of the oriented and disoriented states discussed above (Cooke et al., 1982). Recently, time-resolved EPR studies using caged ATP found a smaller ordered fraction, 11–13% (Fajer et al., 1990). Saturation transfer (ST)-EPR has also been used to monitor the rotational correlation times of the probes attached to cross-bridges and has shown that the correlation times for these bound and detached states are on the order of milliseconds and microseconds, respectively (Thomas et al., 1980). The ST-EPR spectrum of the probes in active fibers could again be interpreted as a linear combination of those seen in rigor and relaxed fibers, with almost the same fraction obtained in conventional EPR studies (Barnett and Thomas, 1989). In the original interpretation of the spectra of active fibers, the disordered probes were thought to be attached to myosin heads that were not attached to actin. More recently, however, measurements of probe mobility with ST-EPR have shown that, in the presence of ATP, myosin can attach to actin in states in which the probes are mobile on the microsecond time scale (Berger et al., 1989; Berger and Thomas, 1993). The observation that mechanical stiffness is proportionally higher than the ordered fraction also suggests that myosin heads are attached to actin in disordered but stiff states (Fajer et al., 1990). Such mobile or disordered states could precede force generation or could also be involved in generating force. The present study was designed to monitor the orientation of possible pre-powerstroke states, in part to determine whether they corresponded to the mobile states seen by ST-EPR or to the disordered states found in active fibers. We find that the probes are highly disordered in states that are stabilized by BDM. A similar result has also been found for states stabilized by a phosphate analogue, aluminum fluoride (AlF_x) (Raucher and Fajer, 1994). This is in marked contrast to the pre-powerstroke state stabilized by P_i, in which the EPR signal in actively contracting fibers does not show an increasing disordered component with increasing concentrations of P_i (Zhao et al., 1995).

MATERIALS AND METHODS

Thin strips of rabbit psoas muscle, 1–2 mm in diameter, were dissected, tied to thin wooden rods with surgical thread, chemically skinned, and stored in a buffer containing 5 mM EGTA, 5 mM magnesium acetate ($MgAc_2$), 0.12 M potassium acetate (KAc), 20 mM N-tris(hydroxymethyl)-methyl-2-aminoethane sulfonic acid (TES), and 50% glycerol, pH 7.0, as described by Cooke and Pate (1985). The measurements of fiber mechanics were made by using the experimental apparatus described by Pate et al. (1994), which permits transferring mounted fibers between wells containing differing experimental buffers. Single fibers were dissected from a small bundle of glycerinated fibers and mounted in a well between a solid-state force transducer (Akers 801; SensoNor, Horten, Norway) and an arm connected to a rapid motor (General Scanning, Watertown, MA) for changing muscle length. Duco cement (Dupont Chemical Co., Wilmington, DE) diluted 1:10 (v/v) in acetone was used as a glue. Buffer was added to the well immersing the fiber. Temperature was maintained by passing temperature-controlled water through the aluminum stage surrounding the well and monitored by a small thermistor adjacent to the force transducer. The length of mounted fiber was measured at ×20 magnification with the graticule of a dissecting microscope mounted directly over the fiber well. The resonant frequency of the transducer with mounted fiber was 4 kHz. Fiber tension was monitored by a 486 personal computer with Tecmar A/D boards (Tecmar Co., Cincinnati, OH). Isometric tension was normalized with respect to fiber area by measuring the fiber diameter at five to seven locations along the fiber at ×126 magnification and averaging the values.

Fiber stiffness was determined from a series of rapid extensions of muscle length of differing magnitudes applied to a fiber. For these measurements, a 1% change in muscle length was 90% complete in 0.5 ms. This corresponds to a speed of stretch of 2×10^3 nm/half sarcomere/s. Fibers were typically stretched by 0.3, 0.6, 0.9, and 1.2% of fiber length, and the peak force was reached after the stretch was determined. The plot of peak force versus the percent length change was linear to a good approximation, and a least-squares linear fit was made to the data. The slope was taken as the fiber stiffness (Pate and Cooke, 1988). Although the stiffness was measured on single fibers and the spectra on bundles, this should not pose a problem. Measurements of stiffness on small bundles of fibers (three to five) provide values that are the same as for single fibers.

For mechanical and EPR experiments, the rigor buffer contained 0.195 M KAc, 3 mM K_2HPO_4, 5 mM $MgAc_2$, 20 mM MOPS, and 1 mM EGTA, pH 7.0. The relaxing buffer contained 0.1 M KAc, 5 mM $MgAc_2$, 3 mM K_2HPO_4, 20 mM MOPS, 25 mM creatine phosphate (CP), 5 mg/ml creatine phosphokinase (CK), and 5 mM ATP, pH 7.0. All experiments were done at 24°C. Fibers were activated by addition of ~1.1 mM $CaCl_2$ (final pCa ~4.5). For all experiments involving activated fibers, after initial activation by addition of Ca^{2+}, small additional aliquots of Ca^{2+} were added to insure that fibers were fully activated (verified by lack of an effect on either isometric tension or the EPR spectra). Some EPR control experiments required increased [CP]. In these experiments, constant ionic strength was maintained by decreasing the [KAc]. The concentrations of the solution ionic species and ionic strength were calculated by using the computer program described in Pate et al. (1991). The final calculated MgATP concentration was 3.5 mM, and ionic strength was 220 mM. BDM (up to 25 mM) was additionally added as required.

Myosin ATPase activities were determined by measurement of the release of inorganic phosphate at 25°C with malachite green (Lanzetta et al., 1979). The K^+-EDTA ATPase activity was assayed in a solution containing 0.6 M KCL, 4 mM EDTA, 50 mM Tris-HCL, pH 7.9, and 0.1 mg/ml myosin. The Ca^{2+}-ATPase activity was assayed in a solution containing 0.6 M KCL, 4 mM $CaCl_2$, 50 mM Tris-HCL, pH 7.9, and 0.1 mg/ml myosin. The Mg^{2+}-ATPase activity was assayed in a solution containing 0.1 M KCL, 4 mM $MgCl_2$, 50 mM TES, pH 7.0, and 0.5 mg/ml myosin with BDM added as required. The reaction was started by adding 1–2 mM ATP to the given solutions, and aliquots were quenched at times from 30 to 120 s (Crowder and Cooke, 1984).

For EPR experiments, the reactive sulfydryl cys-707 (SH-1) in glycerinated rabbit psoas fibers was labeled with *N*-(1-oxyl-2,2,6,6-tetramethyl-4-piperdinyl) maleimide (MSL) by the following procedure. All steps were performed at 0°C. Glycerinated fibers were dissected into small bundles of

25–50 fibers. These were washed in 20 mM MOPS, 5 mM $MgCl_2$, and 1 mM EGTA, pH 7.0 (buffer A), for 20 min to remove the glycerol. The fibers were then incubated for 60 min in buffer A to which 60 μM 2–2′-dithiobis(5-nitropyridine) (NO_2SPY) had been added (preblock step). Fibers were subsequently washed again in buffer A for 10 min, followed by a 10-min equilibration in 0.18 M KAc, 5 mM $MgCl_2$, 5 mM EGTA, and 20 mM 2-(N-morpholino)ethanesulfonic acid (MES), pH 6.5 (buffer B). Fibers were then labeled for 20 min in buffer B, with 0.1 mM MSL and 5 mM $Na_4P_2O_7$ added (the MSL labeling step). Fibers were subsequently washed for 10 min in buffer B to remove unreacted MSL labels and then equilibrated for 40 min in the previously described skinning buffer. Fibers were then stored at −20°C until use. Before experimentation, the fibers were washed with rigor buffer containing 5 mM dithiothreitol (DTT) for 30 min (the unblocking step).

The actual MSL-labeling steps above are similar to those described previously (Thomas and Cooke, 1980). The additional initial preblock step is motivated by the following observations. Fibers are reacted with NO_2SPY under conditions in which SH-1 is only very weakly reactive (low ionic strength, physiological pH). NO_2SPY reacts other SH groups in the fibers, forming disulfide bonds and hence blocking these groups from reacting with MSL during the subsequent steps (high ionic strength, low pH) in which SH-1 is labeled. After the MSL labeling of SH-1, the disulfide bonds formed with NO_2SPY are then removed by washing with DTT, enhancing mechanical function. We note that, in the present protocols, fibers were not reacted with $K_3Fe(CN)_6$ to reduce the EPR signal from nonspecific labeling as has sometimes been the practice in the past. The degree of SH-1 modification was determined by the extraction of fiber myosin and the measurement of the K^+-EDTA ATPase activity as described in Crowder and Cooke (1984). The K^+-EDTA ATPase activity of fiber myosin was 84 ± 5% (three observations) of control after the preblocking step. Subsequent labeling with MSL reduced the K^+-EDTA ATPase activity further to 48 ± 4% (three observations) of control. After treatment with DTT (unblocking step), this activity was slightly increased to 55 ± 5% (three observations) of control. Thus, the labeling procedure resulted in a 40–50% decrease in the K^+-EDTA ATPase activity, indicating that 40–50% of myosin heads were modified. In the control experiments, the K^+-EDTA ATPase activity of preblocked fibers washed by DTT had recovered to its normal value. In the unlabeled fibers also treated with DTT, little or no change in the ATPase activity was found.

MSL probes were mainly attached to the SH-1 group on myosin, although they also reacted to a lesser degree with other SH groups such as SH-2 (cys-697) (Thomas and Cooke, 1980; Crowder and Cooke, 1984). The fraction of modification of SH-1 and other SH groups could be estimated by analyzing the rigor EPR spectrum (Pate and Cooke, 1988). In the EPR rigor spectrum (see Fig. 4 *a*), in which fibers were aligned parallel to the magnetic field, the first and second peaks located at the low field arise from the disordered and ordered probes, respectively. We found that 80% of the probes were ordered and 20% were disordered using the formula given by Pate and Cooke (1988). Assuming that ordered probes were attached to SH-1 and disordered probes were attached to nonspecific groups, the data have suggested that 80% of the probes were attached to SH-1 and 20% were located at other groups such as SH-2. Taken with the K^+-EDTA ATPase activity, this leads to the conclusion that our new labeling procedure resulted in 40–50% of the probes bound to SH-1.

To determine the effect of labeling on the action of BDM, the ATPase activity was measured for purified SH-1-modified myosin. Myosin was purified from myofibrils as described previously (Tonomura et al., 1966) and dissolved in a high salt solution (0.6 M KCL, 50 mM MOPS, pH 6.5). A small amount of MSL solution (10 mM stock solution in dimethylformamide) was added to the myosin (5 mg/ml, 20.8 μM SH-1) to a final concentration of 29 μM, corresponding to 1.4 probes per SH-1. EPR spectra were taken for aliquots of the MSL-myosin solution at different time points to monitor the ratio of the signals from both bound and free MSL probes. After 1 h of labeling on ice, the myosin solution was diluted by adding 10 volumes of cold water, and a myosin pellet was collected after centrifugation at 12,000 *g* for 10 min. The EPR spectra indicated that there were approximately 0.9 labels per myosin head after the reaction.

K^+-EDTA and Ca^{2+}-K ATPase activities were assayed for the above MSL-labeled myosin. We found that K^+-EDTA activity was decreased by 80 ± 3% (three observations), but Ca^{2+}-K ATPase activity was elevated by a factor of 5.2 ± 1.2 (three observations). Double integral of the EPR spectra of labeled myosin showed that the molar ratio of probe to myosin heads was 0.9. Assuming that the probe reacted only with the SH-1 or SH-2 groups on myosin, the above data suggested that the labeling of purified myosin procedure resulted in four subpopulations, corresponding to probes attached to SH-1, SH-2, both, or neither. The fractions of the four populations could be estimated by using the formula given by Crowder and Cooke (1984). We found that 50–60% of myosin heads were labeled on SH-1, 5–10% on SH-2, and 15–20% on both SH-1 and SH-2, and 15–20% were not labeled.

For EPR experiments, MSL-labeled fibers were dissected into small bundles of approximately 15 fibers. These (6–8 total) were accumulated into larger bundles of approximately 100 fibers, pulled into a capillary (0.8 mm inside diameter and 10 mm long), and placed in the center of the TE_{011} cavity (Bruker Instruments, Billerica, MA). The fibers were aligned parallel to the static magnetic field (H_0). The two ends of the fibers in the capillary were secured with surgical thread to prevent length changes. The capillary was attached to a flow system that allowed solutions to flow through and rapidly diffuse into the fibers. The flow speed was approximately 2 cm/s. The division of the experimental bundle into smaller bundles was found to provide better buffer permeation into the larger bundles required for EPR experimentation. During the EPR experiments, a series of spectra was sequentially obtained from each bundle of fibers mounted in the capillary: 1), rigor; 2), relaxed; 3), activated (with or without added BDM); and finally 4), return to the rigor state. A series was considered to be reliable only when the final rigor spectrum duplicated the initial rigor spectrum. The capillary containing the fibers was then removed from the EPR cavity and visually examined under a dissecting microscope to insure that no fibers had broken or come loose from the securing surgical silk during the experiment.

EPR measurements were performed with an ER/200D EPR spectrometer from IBM Instruments (Danbury, CT). X-Band, first derivative absorption EPR spectra were obtained with the following setting: microwave power, 25 mW; gain, 1.0×10^6; center field, 3475 Gauss; time constant, 100 ms; frequency, 9.75 GHz; modulation, 0.8–2 Gauss at a frequency of 100 kHz. Each spectrum used in data analysis represents the average of 20–40 distinct sweeps from an individual experimental preparation. The sweep time was 10 s.

Some principal conclusions of this work were based on a comparison of mechanical measurements with EPR spectroscopy. To minimize differences between the two measurements, each was done by using the same solution and using fibers from the same preparation. All data are given as mean ± SEM except as noted.

RESULTS

Mechanical measurements

The mechanical behavior of glycerinated rabbit psoas fibers was examined as a function of BDM concentration, 0–25 mM. The mechanics of both the MSL-labeled and unlabeled fibers have been measured. For both labeled and unlabeled fibers, mechanical data obtained in the absence of BDM are taken as the control values. Fig. 1 shows a typical time course for isometric tension. A single, unlabeled, glycerinated psoas fiber was initially incubated in relaxing solution. At A, the fiber was activated by adding 1.1 mM $CaCl_2$. At B, the fiber was rapidly transferred to an identical activating solution, which additionally contained 5 mM BDM. At C, the fiber was transferred into another activating solution containing 25 mM BDM. As is evident, the addition of 5 mM and 25 mM BDM caused reductions of 66 and 89%, respectively, in isometric tension when compared with the initial, control value. Finally, at D, the fiber was transferred back to the control

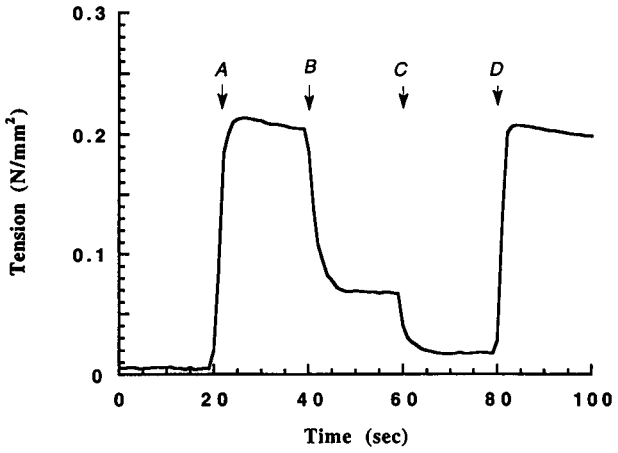

FIGURE 1 Time course of isometric tension of a single glycerinated psoas fiber. The fiber was initially mounted and incubated in relaxing solution. At A, the fiber was activated by addition of Ca^{2+}. At B, after tension stabilized, the fiber was rapidly transferred to an activating solution additionally containing 5 mM BDM and tension decreased by approximately 60%. At C, the fiber was transferred to another experimental well containing an activating solution with 25 mM added BDM and tension again decreased. At D, the fiber was transferred back to the initial (no BDM) activating solution. Tension increased to the control value. Temperature was 24°C.

activating solution. Isometric tension returned to the original level obtained at A, showing that the effects of BDM on mechanics are reversible.

Fig. 2 *a* shows the decrease in isometric tension as a function of increasing BDM concentration for unlabeled psoas fibers and MSL-labeled fibers. Fig. 2 *b* gives mechanical stiffness as determined by rapid length extensions of fibers under identical conditions to Fig. 2 *a*. As is evident from Fig. 2, an approximately 50% reduction in force is obtained at 5 mM BDM; at 25 mM BDM, isometric force is almost completely eliminated (~10% of control). Stiffness does not decrease as rapidly as tension with increasing [BDM], as shown in greater detail in Fig. 3. Here stiffness is plotted as a function of tension for increasing concentrations of BDM from Fig. 2 (both quantities normalized relative to the value obtained for no added BDM). Triangles and circles represent labeled and unlabeled fibers, respectively. For reference, the line of unitary slope, which would occur if tension and stiffness decreased in equal proportion, is also included. For both labeled and MSL-labeled fibers, the data clearly are above the line, showing that stiffness decreases to a lesser extent than tension. The sarcomere length has not been measured in these experiments; thus, the values of stiffness are lower than the true cross-bridge stiffness because of the end compliance of the fiber. However the presence of end compliance, which has been shown to be nonlinear, will act to decrease the apparent stiffness as fiber force is decreased; e.g., the apparent stiffness of rigor fibers increases as the tension increases. Thus, if anything, the stiffness measurements will underestimate the fraction of attached cross-bridges as the concentration of BDM is raised.

Comparing unlabeled fibers and MSL-labeled fibers in the absence of added BDM, isometric tension and mechanical

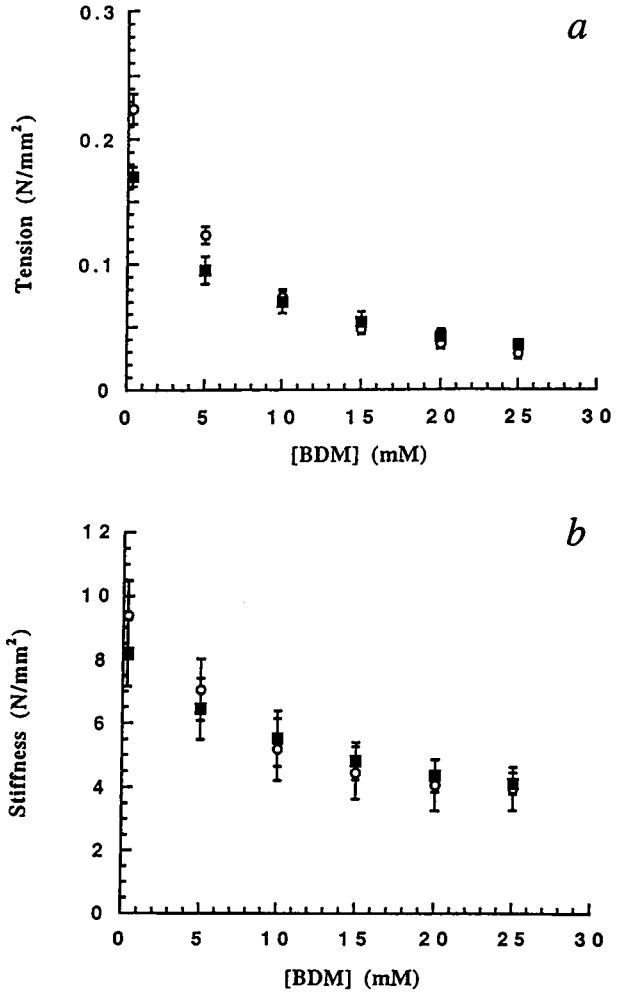

FIGURE 2 (*a*) Isometric tension and (*b*) isometric stiffness as a function of BDM concentration obtained from fully activated single psoas fibers. ○, unlabeled fibers; ■, MSL-labeled fibers, with the fibers taken from the same preparation of chemically skinned fibers represented by open circles. Fiber stiffness was determined by using a series of rapid extensions of fiber length. Each data point represents an average of 7–10 fibers. Errors are SEM.

stiffness are lower in the MSL-labeled fibers. Mean values are reduced by 24 and 14%, respectively. For 10 mM BDM, however, no statistically significant difference in tension or stiffness is observed when MSL-labeled and unlabeled, control fibers are compared. The degradation of mechanical function in the SH-1-labeled fibers in the absence of BDM is comparable with that observed previously for psoas fibers with a comparable degree (50–60%) of SH-1 modification (Crowder and Cooke, 1984).

EPR spectroscopy

A series of conventional EPR spectra from a bundle of MSL-labeled fibers held isometrically in a capillary and oriented parallel to the magnetic field are shown in Fig. 4. Fig. 4 *a* is for rigor conditions, in which cross-bridges are tightly bound to actin. The three sharp central peaks indicate a highly ordered component arising from the MSL probes attached to cys-707. It implies that rigor cross-bridges, or at

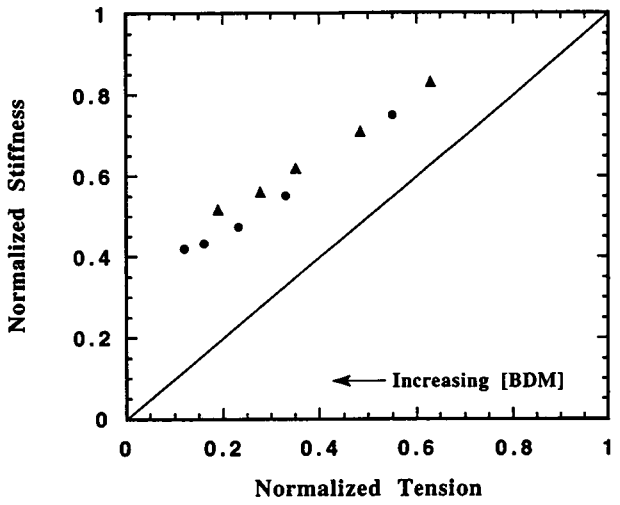

FIGURE 3 Normalized tension versus normalized stiffness as a function of BDM concentration. The tension and stiffness are normalized to those obtained in the absence of BDM for labeled (▲) and unlabeled (●) fibers, respectively. The solid line is that to be expected if tension and stiffness decrease by equivalent amounts. The plot shows that isometric tension decreases more rapidly than mechanical stiffness as BDM concentration increases.

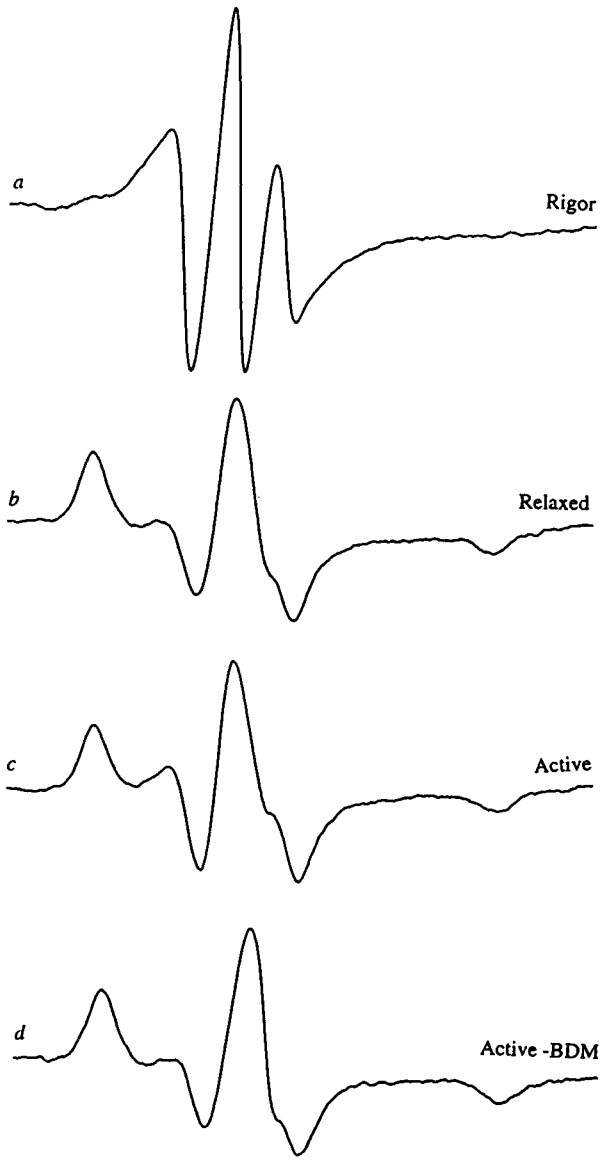

FIGURE 4 EPR spectra from rabbit psoas fibers with the MSL probe covalently attached to cys-707 (SH-1) of the myosin cross-bridges. The derivative of absorption is plotted as a function of magnetic field. Approximately 100 labeled fibers were located in a capillary that was aligned parallel to the magnetic field. The baseline for each spectrum is 100 Gauss wide. The EPR spectra were obtained in the following conditions: (*a*) rigor, (*b*) relaxation, (*c*) isometric contraction in the absence of added BDM, and (*d*) isometric contraction in the presence of 25 mM BDM. The temperature was 24°C.

least that portion near cys-707, are highly ordered with respect to the magnetic field. The orientation distribution of these probes can be described by a Gaussian distribution at an angle of 82° from the fiber axis, with a full width at half maximum of 12–15°. Similar results for MSL-labeled fibers have been previously reported (Thomas and Cooke, 1980).

The spectrum shown in Fig. 4 *a* contains an additional small peak at low field (shoulder at left of first peak), corresponding to an isotropic distribution of probes. These correspond to nonspecific labeling of other sites in the filament array (Thomas and Cooke, 1980). An important observation is that the magnitude of this peak is significantly reduced when compared with that produced by previously employed MSL labeling protocols. These protocols generally required the additional incubation of fibers in a buffer containing $K_3Fe(CN)_6$. This had proven necessary to reduce sufficiently the nonspecific signal to obtain resolution in the low field, ordered peak. We can now obtain this specificity via the preblocking step, with the added advantage that the preblock can be removed by mild treatment with DTT after MSL labeling. The treatment of fibers with $K_3Fe(CN)_6$ is known to be deleterious to fiber mechanics, resulting in up to a 40% reduction in isometric tension when compared with unlabeled control fibers (Fajer et al., 1988). In contrast, the 1-h preblock step followed by DTT treatment yields fibers that produce 96 ± 5% (10 observations) of the isometric tension generated by untreated, control fibers.

When relaxing buffer is flowed through the fibers, cross-bridges detach from actin, undergoing rapid, random Brownian motions. The EPR spectrum from relaxed fibers (Fig. 4 *b*) shows that the angular distribution of probes is isotropic (Thomas and Cooke, 1980; Barnett et al., 1986). The EPR spectrum obtained from the MSL-labeled fibers during active, isometric contraction (no added BDM) is shown in Fig. 4 *c*. Interpreting the active spectrum as a linear combination of the rigor and relaxed spectra, least-squares fits show that the fraction of oriented probes (rigor spectrum component) is 17 ± 1.5% (eight observations) that of the total active, isometric signal. The residual of this fit was flat to within experimental error. The ordered fraction is slightly less than the value of 20% reported previously by this lab with other labeling protocols and is a little greater than the 11–13% fraction found by Fajer et al. (1990). Fig. 5 *a* shows the correspondence between the rigor spectrum and the ordered

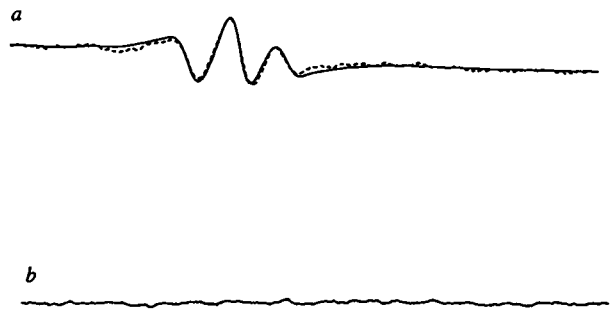

FIGURE 5 Difference spectra from Fig. 4. (*a*) The solid line is the difference spectrum calculated as active contraction (Fig. 4 *c*) minus 0.82 times relaxed spectrum (Fig. 4 *b*). The dashed line is calculated as 0.18 times rigor spectrum (Fig. 4 *a*). (*b*) A similar difference spectrum calculated from active contraction in the presence of 25 mM BDM (Fig. 4 *c*) minus relaxed spectrum (Fig. 4 *b*). No ordered component is seen in Fig. 4 *b*, showing that the probes were completely disordered in 25 mM BDM.

component of active spectra in greater detail. The solid line is 0.18 times the rigor spectrum (Fig. 4 *a*); the dashed line is the difference spectrum obtained by subtracting 0.82 times the relaxed spectrum (Fig. 4 *b*) from the active spectrum (Fig. 4 *c*). The correspondence between the two spectra shown indicates that, for active contraction with no added BDM, approximately 82% of the cross-bridges are disordered and 18% are ordered. The spectral shape of the ordered component of the active fibers is statistically indistinguishable from the ordered component of rigor fibers. For these particular spectra, the fractional values are close to the mean fractional values obtained over the entire set of eight experiments. With the improved labeling protocols, we also see the same angular orientation in active fibers as is seen in rigor; i.e., no new angular cross-bridge orientations at the SH-1 site are introduced during isometric contraction as has been observed previously (Cooke et al., 1982).

When 25 mM BDM was included in the activating solution, the peaks associated with ordered probes disappeared, and the spectrum returned to one that resembled that seen in relaxed fibers. Addition of 25 mM BDM to relaxed fibers also caused no change in the relaxed spectrum. Thus, in the presence of BDM and ATP, the probes were disordered in both the presence and absence of Ca^{2+}. Addition of 25 mM BDM to rigor fibers caused no change in the rigor EPR spectrum, indicating that this EPR spectral change requires the presence of myosin-bound nucleotides or these nucleotides plus calcium. When the spectra of active fibers in 25 mM BDM were analyzed as a combination of the spectra obtained in rigor and relaxation, we obtained an ordered component of 1.1 ± 1.6% (eight observations). Thus, the ordered fraction obtained in active fibers with 25 mM BDM is not statistically different from that obtained during relaxation. It is likewise not different from the 1.7% that would be expected from the 10% residual isometric tension at 25 mM BDM (Fig. 2), assuming that the ordered component scaled linearly with the tension. Fig. 5 *b* shows the difference spectrum obtained by subtracting the active spectrum obtained in 25 mM BDM (Fig. 4 *d*) from the relaxed spectrum (Fig. 4 *b*). The resultant difference spectrum is flat to within our experimental error in agreement with the above least-squares analysis.

In active fibers, the ATPase rate is significantly increased relative to the relaxed state. Thus,the possibility exists that some fraction of the ordered component of the active fiber spectrum results from inadequate buffering of internal MgATP concentrations and the formation of a rigor core in the fiber bundles. The ATP, CP, and CK levels used in these experiments have been shown previously to be sufficient to buffer substrate concentrations in single fiber mechanics experiments (Cooke and Bialek, 1979) at a lower temperature, 10°C. In the present experiments, however, an aggregate bundle of ~100 fibers, itself composed of individual smaller bundles of ~15 fibers, is being used. Our conclusions rest on the verification of adequate internal buffering of MgATP. This question has been addressed by examining the ordered component of the active spectrum as a function of [CP], holding [ATP] at 5 mM. We note that CP has a diffusion coefficient in muscle fibers that is approximately twice that of ATP (Meyer et al., 1984) and, thus, in the presence of adequate concentrations of CK can be a more effective method for delivering high energy phosphate to the center of a fiber bundle (via rephosphorylation of ADP generated by the actomyosin ATPase internal to the fiber bundle) than is the alternative method of increasing the concentration of substrate, ATP. Fig. 6 shows the mean ordered fractions in active fibers as a function of [CP + ATP] at constant ionic strength and a piece-wise linear fit to the data. As discussed later, the data in Fig. 6 are expected to be piece-wise linear from theo-

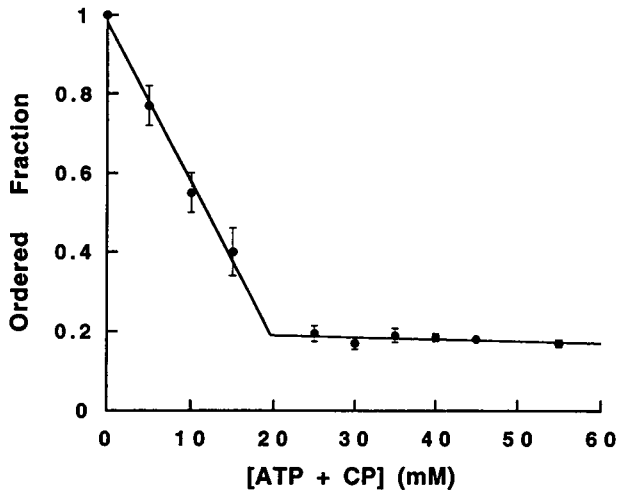

FIGURE 6 The mean ordered EPR fraction seen in active fibers as a function of [CP + ATP]. [ATP] was 5 mM for all data points. Data are mean ± SEM for three to eight observations per point. Ionic strength was held constant at 220 mM by varying KAc concentration. Least-squares linear fits show a biphasic ordered fraction, linearly decreasing as [CP + ATP] increases to approximately 20 mM and constant for concentrations greater than 20 mM. The slope of the least-squares fit for [CP + ATP] > 25 mM is not statistically different from zero, indicating that in this region there is no rigor core in the fiber bundles. The data in Fig. 4 are for 30 mM [CP + ATP], on the flat portion of the plot.

retical considerations (see Appendix). The mean ordered fraction decreases linearly for [CP + ATP], increasing up to approximately 20 mM. For 25 mM [CP + ATP], the decrease in the ordered fraction levels off as [CP + ATP] increases. Indeed, the slope of the least-squares, linear fit to the data for [CP + ATP] in the range 25–55 mM has a slope of $-5.2 \times 10^{-3} \pm 6.0 \times 10^{-3}$ mM^{-1}. Thus, the ordered fraction is not statistically different from uniform in this region. The spectra presented in Fig. 4 were obtained in the saturated regime ([CP + ATP] = 30 mM).

Mg^{2+}-ATPase activity of MSL-labeled myosin

Previous biochemical studies have shown that, at high levels of BDM (> 20 mM), the Mg^{2+}-ATPase activity is decreased by approximately 70–80% (Herrmann et al., 1992; Higuchi and Takemori, 1989). However, the effect of BDM on the Mg^{2+}-ATPase activity of MSL-labeled myosin has not been determined previously. Thus, we examined the Mg^{2+}-ATPase activity of MSL-labeled myosin in the absence and the presence of BDM at 24°C. In the absence of BDM, the activity was 0.48 ± 0.10 s^{-1}, which is approximately 10 times larger than that of normal myosin in agreement with previous results (Sleep et al., 1981). Upon addition of 25 mM BDM, this activity was decreased to 0.12 ± 0.06 s^{-1}, approximately 25% from control. Thus, the inhibition of the Mg^{2+}-ATPase activity is almost the same in control and labeled samples. Although the labeled myosin is heterogeneous, the results still lead to the conclusion that the action of BDM is not altered by labels at the SH-1. The double integral of the EPR signal showed that there were 0.9 labels attached per myosin head. Although some myosin heads will have labels at both SH-1 and SH-2, their Mg^{2+}-ATPase activity will be completely inhibited in both the presence and absence of BDM. Because the Mg^{2+}-ATPase activity of SH-1-labeled myosin is 10 times larger than that of unlabeled myosin, and the majority of the myosins are labeled at the SH-1, our measurements are dominated by the activity of SH-1-labeled myosin. The observation that the effect of BDM is similar for unlabeled and labeled myosin thus leads to the conclusion that labels at the SH-1 have little effect on the action of BDM.

DISCUSSION

The generation of force and motion by motor proteins must of necessity involve large changes in their conformation. A complete understanding of the nature of these conformational changes would require resolution of at least two different structures, the structure at the beginning of the powerstroke and that at its end. One of these structures, the structure of the rigor actomyosin complex, which occurs at the end of the powerstroke, is now relatively well established. In the absence of ATP, actin and myosin form a very tight complex, and a variety of kinetic and chemical experiments have suggested that this complex occurs at the end of the powerstroke.

Although the rigor complex has been relatively easy to study, the structures of other acto-S1 complexes have presented more problems. A major difficulty is that many of these states can be observed only as transient intermediates in the cycle of interactions. An approach to this problem is to use conditions that increase the population of one of these states. In this paper, we have used a small molecule, BDM, to selectively stabilize one putative pre-powerstroke state. Binding of the molecule to the myosin head has been shown to inhibit the rate of P_i release and to accelerate the rate of ATP hydrolysis (Herrmann et al., 1992), thus stabilizing a myosin·ADP·P_i complex. We have monitored the orientation of cross-bridges in this complex bound to actin by paramagnetic probes attached to a reactive sulfhydryl, cys-707. This residue is located in the catalytic domain on the side opposite from the nucleotide site.

Does BDM have similar effects on labeled and unlabeled heads? Fig. 2 shows that BDM suppresses the mechanical function for both unlabeled and MSL-labeled fibers by similar amounts. However, because MSL-labeled fiber contains both labeled and unlabeled myosin heads, it is not clear that the suppression of mechanics of MSL-labeled fiber is caused by the effects of BDM on unlabeled heads only or on both unlabeled and labeled heads. Fig. 2 *a* shows that, in the absence of added BDM, the isometric tension of MSL-labeled fibers is 0.17 N/mm^2, which is 25% lower than the 0.22 N/mm^2 measured for unlabeled fibers. Because the MSL-labeled fiber contains approximately 50% unlabeled myosin heads that should generate 0.11 N/mm^2 tension, the MSL-labeled myosin will produce 0.06 N/mm^2. Thus, the tension generated by a labeled head is approximately one-half that of an unlabeled head. At 25 mM BDM, the tension of an unlabeled fiber is 0.033 N/mm^2, 15% of the tension in the absence of BDM. Assuming the same amount of suppression by BDM for the tension generated by unlabeled heads in MSL-labeled fibers, the 50% of unlabeled heads should produce 0.017 N/mm^2 in the MSL-labeled fiber at 25 mM BDM. Together with the 0.035 N/mm^2 observed in the MSL-labled fiber at 25 mM BDM, one can calculate that the MSL-labeled myosin will generate 0.018 N/mm^2. Therefore, 25 mM BDM has decreased the tension of the labeled heads from 0.06 to 0.018 N/mm^2, a 70% decrease that is similar to the 85% inhibition seen for unlabeled heads. A similar result is obtained from the analysis of the stiffness data. We find that addition of 25 mM BDM reduces stiffness by 30 and 57% for labeled and unlabeled heads, respectively. The conclusion that the effect of BDM is not greatly altered by labeling is supported by the observation that the effect of BDM on the Mg^{2+}-ATPase activity of purified myosin is similar for labeled and unlabeled myosin. The effect of BDM on myosin kinetics may explain why BDM has similar actions on labeled and unlabeled fibers. Binding of BDM to unlabeled myosin has been shown to elevate the rate of the ATP hydrolysis step and to inhibit the subsequent release of P_i. This faster rate of hydrolysis will counteract the inhibition of this step by labeling, producing cross-bridge populations that are more similar to unlabeled fibers.

The observation that stiffness is inhibited to a significantly more reduced extent than is isometric tension suggests that

the myosin·ADP·P_i complex does attach to the actin filament. The fraction of myosin heads that are attached to actin in the presence of BDM is not known exactly. However, one can make some estimates from the value of stiffness. In 25 mM BDM, the fiber stiffness is about one-half that observed in the absence of BDM. As it is unlikely that the pre-powerstroke state is more stiff than states later in the powerstroke, one can assume from the stiffness measurements that at least one-half of the cross-bridges that were attached in the absence of BDM remain attached in the presence of 25 mM BDM. It is clear from the spectra shown in Figs. 4 and 5, however, that one-half of the 17% ordered fraction seen in active fibers in the absence of BDM is not observed in the presence of BDM. From this one can conclude that, in the presence of BDM, the cross-bridges are attached to actin but that the paramagnetic probes attached to cys-707 are highly disordered.

Does probe disorder imply that the whole of the catalytic domain is also disordered, or could it arise from disorder of the probe relative to the protein? We know that the probe is ordered relative to the protein in the rigor state. A previous investigation showed that the mobility of the probe was not changed when ATP was added to immobilized myosin heads, suggesting that the interaction between protein and probe was not changed (Thomas et al., 1980). The observation that BDM caused no change in the spectrum of relaxed fibers likewise suggests that it has not altered this interaction either. However, the region that contains cys-707 must undergo significant structural changes to allow cross-linking to occur between cys-707 and cys-697 (Rayment et al., 1993a). Thus, we conclude that the most probable interpretation of the data is that the catalytic domain is itself disordered in the presence of BDM. However, the possibility that some of the disorder arises from disorder of the probe relative to the protein cannot be completely excluded.

Studies of spectroscopic probes have previously shown that myosin heads can be attached to actin in states that display microsecond mobility. Berger and Thomas (1993) measured the rotational mobility of myosin heads in myofibrils using the same paramagnetic probe as studied here. Previous work had shown that myosin heads in rigor fibers are immobile, with correlation times longer than 100 μsec but that they are mobile with correlation times on the order of 1–10 μsec in relaxed fibers and myofibrils (see Thomas, 1987, for review). Berger and Thomas (1993) found that, in myofibrils undergoing isometric contractions, the probes displayed a large degree of rotational mobility. As an independent measure of the fraction of heads attached to actin, they determined the proteolytic susceptibility of the 20–50K junction. This is a flexible region of polypeptide chain thought to be involved in the formation of the actomyosin bond and protected from proteolysis when myosin is bound to actin (Chen and Reisler, 1984). They found that the immobile fraction of myosin heads was smaller than the fraction bound to actin as determined by proteolysis. This result then agreed with earlier results obtained with purified actin and S1. These studies also found that the fraction of myosin heads shown to be attached to actin via sedimentation was larger than the fraction of myosin heads that was immobilized by its interaction with actin (Berger and Thomas, 1989). Together these results suggested that myosin could attach to actin in states that were mobile, and presumably disordered, although disorder was not measured in these experimental preparations. The present results show that myosin can also attach to actin in states that are highly disordered. Although Thomas and co-workers measured probe mobility, the degree of disorder engendered by this mobility was not known, nor could it be determined which states in the cycle were disordered and mobile and which states were ordered and presumably immobile. The present work suggests that the mobility observed by Thomas and co-workers was that of states that were early in the powerstroke or were pre-powerstroke states and that the degree of disorder in these states was very high.

The structures of several cross-bridge states that are likely to occur before the powerstroke have been studied by various approaches. These states fall into three rough groups. Nucleotide analogues have been used to stabilize states resembling actin·myosin·ATP. Phosphate analogues and BDM have been used to stabilize states resembling actin·myosin·ADP·P_i, and relaxed fibers at low ionic strength stabilize weakly bound states in which a stronger actomyosin interaction is prevented by the regulatory proteins. Results obtained from these states have varied, as discussed below.

One possible pre-powerstroke state is that obtained in relaxed fibers at low temperatures and low ionic strengths (Brenner et al., 1982; Yanagida et al., 1982; Brenner, 1987). X-ray diffraction has shown that the structure of this state is different from that obtained in rigor (Yu and Brenner, 1989). Paramagnetic probes attached to cys-707 display some degree of order in these fibers, with an angular distribution that is centered at the same angle as that in rigor but that has a wider spread of angles, up to 40°, as compared with the 12° spread seen in rigor fibers (Fajer et al., 1991). The nucleotide bound to myosin in these states is likely to be a mixture of ATP and ADP·P_i.

A state with bound triphosphates can be obtained using ATP analogues. Two nucleotides, ATPγS and GTP, are hydrolyzed very slowly, and both may arrest the cross-bridges in states that would resemble the myosin triphosphate state (Dantzig et al., 1988; Pate et al., 1993). In the absence of Ca^{2+}, both of these nucleotides relax fibers. However, in the presence of Ca^{2+}, the fibers generate little or no tension, whereas fiber stiffness increases to values similar to those obtained in fibers activated in the presence of ATP. This state differs from the low ionic strength relaxed state, in that it is obtained in the presence of Ca^{2+} instead of in its absence, and the frequency dependency of stiffness shows that equilibrium between attached and detached states occurs on a slower time scale (Dantzig et al., 1988). Paramagnetic probes attached to cys-707 in fibers activated in the presence of GTP resemble those activated in the presence of ATP (Pate et al., 1992). That is to say, there is an approximately 20% rigor-like component that appears in the spectrum upon activation. A similar result is also obtained in the presence of ATPγS (P. Fajer,

unpublished). Thus, it would appear that in these states the catalytic domain of myosin is bound to actin at the same orientation as that found in rigor.

In the presence of AlF_x, ATP, and Ca^{2+}, the cross-bridges are trapped in a pre-powerstroke state in which AlF_x has replaced P_i (Chase et al., 1993). Under this condition, a fiber displays 40% of control stiffness without generating force (Chase et al., 1993). EPR spectroscopy showed that cross-bridges in the pre-powerstroke state trapped by AlF_x are highly disordered but that they are also immobile (Raucher and Fajer, 1994). The disorder is equivalent to that seen in the present study in the presence of BDM. Similar disorder in the presence of BDM was observed with x-ray diffraction from living frog fibers by Yagi et al. (1992). Together these three results could lead one to the conclusion that states involving actin·myosin·ADP·P_i are disordered. However, this state can also be achieved in the presence of high levels of P_i, which rebinds to the nucleotide site on the cross-bridge, reversing the powerstroke (Hibberd et al., 1985; Hibberd et al., 1986). In contrast to the results from AlF_x and BDM (this work), however, probes attached to cys-707 show that cross-bridges in the pre-powerstroke state achieved by high [P_i], at both high and low pH, are ordered, with the same orientation seen in rigor (Zhao et al., 1995). Thus, it appears that the states involving bound P_i, or P_i analogues, can exhibit different degrees of order at cys-707, depending on how the state is attained. Why are the states stabilized by the analogues different from those stabilized in high P_i? One explanation is that they are intermediates that are only briefly populated in the native cycle.

The observation of almost isotropic disorder in a myosin head that is bound to actin, as we see in the presence of BDM, requires that the bond between actin and myosin be exceptionally flexible. The proposal of Rayment et al. (1993b) that a weak bond can occur via the electrostatic attraction between two stretches of peptide chain, one of which is so disordered that it is not observed in the crystal, could provide for such flexibility. Such states may explain the mobile heads found attached to actin during steady-state cycling (Berger and Thomas, 1993).

Two questions remain unanswered concerning the disordered heads attached to actin. What is their population in normal active fibers, and what role do they play in force generation? The exact fraction of myosin heads bound to actin in active fibers remains controversial. The stiffness of an active fiber, which is one measure of cross-bridge attachment, is 75% of that of a rigor fiber (Goldman and Simmons, 1984). Although stiffness has often been used as a measure of cross-bridge attachment, and the high stiffness observed in the fibers in the presence of BDM certainly indicates that a considerable fraction of cross-bridges are attached to actin, stiffness is unlikely to be linearly related to the fraction of myosin heads attached to actin (Pate and Cooke, 1988). Previous work has shown that a myosin molecule attached by one head to actin is probably as stiff as one attached by both heads, suggesting that the fraction of attached heads that contribute to fiber stiffness may be closer to 37% (Pate and Cooke, 1988; Fajer et al., 1988). This number, however, is still larger than the 15–20% of myosin heads that have ordered probes at cys-707 or the 25% of myosin heads that are protected from proteolysis (Dong and Reisler, 1989). The observation of disordered, attached heads that are contributing to fiber stiffness as observed in the present work and by Roucher and Fajer (1994) provides an explanation for why the estimate of the fraction of attached heads obtained from measurements of fiber stiffness is higher than that obtained from probe order. The comparison of these two measurements would suggest that the fraction of attached but disordered heads in active fibers is considerable, of the order of 20% for the labeled heads observed in these experiments.

Do any of these disordered states generate force? In the model proposed by Rayment, Holmes, and their co-workers, the large distal catalytic domain of the myosin head binds rigidly to the actin filament during the force-generating steps. Conformational changes within the nucleotide pocket are hypothesized to subsequently drive the rotation of the neck region of myosin (Rayment et al., 1993b). This suggests that the force-generating heads would have ordered probes attached to cys-707. The population of such probes is small in active fibers; however, recent mechanical measurements have also suggested that the population of force-generating heads may be small. The force generated by a single myosin molecule has been estimated to be 3.5–5 pN (Finer et al., 1994). The average force per myosin head in an active fiber can be estimated to be approximately 1.2 pN, suggesting that as few as 25% of the heads may be generating tension at any given time. This estimate is compatible with the concept that all of the force-generating heads have ordered probes on cys-707. In addition, none of the disordered states observed to date appear to be force generating. Although a number of arguments suggest that force is generated only by the heads with ordered probes, the uncertainties in the estimates discussed above leave room for some force generation by disordered heads as well.

In summary, an understanding of the nature of the initial pre-powerstroke state(s) remains a crucial, unresolved question in our analysis of the actomyosin, chemomechanical interaction. In the present study, we have used BDM, an uncompetitive inhibitor of the actomyosin ATPase. The binding of BDM is thought to stabilize a pre-powerstroke actin·myosin·ADP·P_i state. We found that, in the presence of 25 mM BDM, isometric tension is almost totally abolished although mechanical stiffness remained high. This indicates that, in the presence of BDM, myosin heads remained attached to actin but did not generate force. Concurrent application of EPR spectroscopy was used to monitor the structure of the myosin head in the vicinity of SH-1 for this pre-powerstroke state. In active contraction, the EPR spectra indicate an ordered fraction of cross-bridges, presumably from powerstroke states. In the presence of 25 mM BDM, the EPR probes become as disordered as is observed in relaxed fibers in the absence of BDM. Thus, we conclude that the portion of the myosin cross-bridge in the vicinity of SH-1 is disordered in the BDM-stabilized, actin·myosin·ADP·P_i

pre-powerstroke state. Such a state most probably is an intermediate in which myosin attaches weakly to actin before forming a more rigid attachment in which force is produced.

APPENDIX

To determine whether the fibers were adequately supplied with substrate, we measured the ordered fraction as we varied [CP + ATP]. The data, shown in Fig. 6, demonstrated that the ordered fraction in the EPR spectra of active fibers can be approximated in a piece-wise linear fashion. When the concentration of ATP plus CP is less than approximately 20 mM, the ordered fraction decreases in an approximately linear fashion as [ATP + CP] is increased. But for 25 mM [ATP + CP], the ordered fraction remains constant. This Appendix is to demonstrate that the observed piece-wise linear fitting of the ordered fraction in Fig. 6 is actually to be expected and can be explained as follows. A rigor core (and thus an artificially large ordered component to the EPR spectra) occurs in the center of a fiber bundle when there is inadequate diffusion of ATP (or ATP plus CP in the presence of CK) into the center of the fiber bundle. This process can be simulated by using a simple model of diffusion. Assume an external buffer [ATP + CP] equal to C_0. Then, at steady-state, the concentration $C(r)$ of high energy phosphates internal to the fiber bundle can be expressed as (Cooke and Pate, 1985):

$$C(r) = Co - k(\alpha^2 - r^2)/4D, \quad (1)$$

where α is the fiber bundle diameter, $r \leq \alpha$ is the radial distance from the center ($r = 0$) of the fiber bundle, D is the diffusion coefficient of high energy phosphates, and k is the fiber ATPase rate. $C(r)$ is equal to C_0 at $r = \alpha$, and it decreases as r decreases. If C_0 is sufficiently small relative to $kO^2/4D$, the value of $C(r)$ becomes zero at some value of r. We shall take this to define the radius of the rigor core. (The fiber ATPase rate is actually a function of substrate at extremely low levels of [MgATP], but for mathematical simplicity it is taken here to be a constant. For physically realistic parameters, the negative concentrations permitted by Eq. 1 within this region imply that $C(r)$ is actually very small and do not change our conclusions). Thus, to a first approximation, Eq. 1 implies that, if the external concentration, C_0, is sufficiently small, $C(r)$ will be approximately zero (i.e., a rigor core) for $r \leq R$, where:

$$R^2 = \alpha^2 - 4DC_0/k. \quad (2)$$

This result is obtained by solving Eq. 1 for $C(r) = 0$.

For the cylindrical geometry of the fibers in the capillary, the volume of the rigor core is $\pi R^2 L$, where L is the length of fiber. The component of the ordered fraction in Fig. 6 resulting from the rigor core will be proportional to the volume of the rigor core. Hence, it will be proportional to R^2 and, via Eq. 2, it will also be proportional to $\alpha^2 - 4DC_0/k$. Consider a fixed fiber bundle (i.e., a fixed radius a), under conditions in which C_0 is sufficiently small for there to be a rigor core. In this case, as the external concentration C_0 decreases, R^2, and hence the volume of the rigor core increase linearly with C_0. If, however, C_0 is sufficiently large, $C(r) > 0$ for all r, and there is no rigor core. In this regime, increasing C_0 does not affect the ordered fraction.

From Eq. 1, the break point between these two distinct regimes occurs when $C_0 = k\alpha^2/4D$. This external concentration can be estimated from literature values. We take k = 5/s/myosin head (Wilson et al., 1995), a fiber myosin head concentration of 220 μM, and $D = 3 \times 10^{-6}$ cm^2/s (Meyer et al., 1984). We also take α = 0.13 mm, the approximate radius of the fiber bundles inserted into the cavity. The value for α can also be established from the fact that, in our experiments, the 0.4-mm radius capillary is filled with a~ pproximately seven smaller fiber bundles. It is a well known geometrical property that seven circles (e.g., coins) of radius α form an approximate circle of radius 3α when arranged with one of the seven circles in the center, surrounded by the remaining six. Substituting, we calculate C_0 = 15 mM. This value is close to the value of 20 mM observed in Fig. 6. Obviously, simplifying assumptions have been made in the mathematical analysis of the biphasic nature of the ordered component of the active spectra. Nonetheless, theory and experiment appear to be in both qualitative and quantitative agreement.

The authors acknowledge stimulating discussions with E. Pate.
This work was supported by grant AR30868 and AR42895 from the United States Public Health Service (R.C.) and National Institutes of Health biochemistry training grant 5T32CA09270 (L.Z.)

REFERENCES

Bagni, M. A., G. Cecchi, F. Colomo, and P. Garzella. 1992. Effects of 2,3-butanedione monoxime on the crossbridge kinetics in frog single muscle fibers. *J. Muscle Res. Cell Motil.* 13:516–522.

Barnett, V. A., P. Fajer, C. F. Polnaszek, and D. D. Thomas. 1986. High resolution detection of muscle cross-bridge orientation by electron paramagnetic resonance. *Biophys. J.* 49:144–146.

Barnett, V. A., and D. D. Thomas. 1987. Resolution of conformational states of spin-labeled myosin during steady-state ATP hydrolysis. *Biochemistry.* 26:314–323.

Barnett, V. A., and D. D. Thomas. 1989. Microsecond rotational motion of spin-labeled myosin heads during isometric muscle contraction. *Biophys. J.* 56:517–523.

Belknap, B., H. D. White, E. Pate, and R. Cooke. 1993. 2,3-butanedione monoxime (BDM) has similar effects on nucleotide triphosphate hydrolysis in solution and on the mechanical properties of muscle fibers. *Biophys. J.* 64:A24.

Berger, C. L., E. C. Svensson., and D. D. Thomas. 1989. Photolysis of a photolabile precursor of ATP (caged ATP) induces microsecond rotational motions of myosin heads bound to actin. *Proc. Natl. Acad. Sci. USA.* 86:8753–8757.

Berger, C. L., and D. D. Thomas. 1993. Rotational dynamics of actin-bound heads in active myofibrils. *Biochemistry.* 32:3812–3821.

Blanchard, E. M., G. L. Smith, D. G. Allen, and N. R. Alpert. 1990. The effect of 2,3-butanedione monoxime on intial heat, tension, and aequorin light output of ferret papillary muscle, *Pflügers Arch.* 416:219–221.

Brenner, B. 1987. Mechanical and structural approaches to correlation of cross-bridge action in muscle with actomyosin ATPase in solution. *Annu. Rev. Physiol.* 49:655–672.

Brenner, B., M. Schoenberg, J. M. Chalovich, L. E. Greene, and E. Eisenberg. 1982. Evidence for cross-bridge attachment in relaxed muscle at low ionic strength. *Proc. Natl. Acad. Sci. USA.* 79:7288–7291.

Burghardt, T. P., T. Ando, and J. Borejdo. 1983. Evidence for cross-bridge order in contraction of glycerinated skeletal muscle. *Proc. Natl. Acad. Sci. USA.* 80:7515.

Chase, B. P., D. A. Martyn, M. J. Kushmerick, and A. M. Gordon. 1993. Effects of inorganic phosphate analogues on stiffness and unload shortening of skinned muscle fibers from rabbit. *J. Physiol.* 460:231–246.

Chen, T., and E. Reisler,. 1984. Tryptic digestion of rabbit skeletal myofibrils: an enzymatic probe of myosin cross-bridges. *Biochemistry.* 23: 2400–2407.

Cooke, R. 1986. The mechanism of muscle contraction. *CRC Crit. Rev. Biochem.* 21:53–118.

Cooke, R., and W. Bialek. 1979. The contraction of glycerinated muscle fibers as a function of the ATP concentration, *Biophys. J.* 28:241-258.

Cooke, R., M. S. Crowder, and D. D. Thomas. 1982. Orientation of spin labels attached to cross-bridges in contracting muscle fibers. *Nature.* 30: 776–778.

Cooke, R., K. Franks, G. Luciani, and E. Pate. 1988. The inhibition of rabbit skeletal muscle contraction by the hydrogen ions and phosphate. *J. Physiol.* 395:77–97.

Cooke, R., and E. Pate. 1985. The effects of ADP and phosphate on the contraction of muscle fibers. *Biophys. J.* 48:789–798.

Crowder, M. C., and R. Cooke. 1984. The effect of sulphydryl modification on the mechanics of fiber contraction. *J. Muscle Res. Cell Motil.* 5:131-146.

Dantzig, J. A., J. W. Walker, D. R. Trentham, and Y. E. Goldman. 1988. Relaxation of muscle fibers with adenosine 5'-[γ-thio]triphosphate (ATP-[γS]) and by laser photolysis of caged (ATP[γS]): evidence for Ca^{2+}-

dependent affinity of rapidly detaching zero-force cross-bridges. *Proc. Natl. Acad. Sci. USA.* 85:6716–6720.

Dong, A. H., and E. Reisler. 1989. Binding of myosin to actin in myofibrils during ATP hydrolysis. *Biochemistry.* 28:1307–1313.

Fajer, P. G., E. A. Fajer, and N. J. Brunsvold, and D. D. Thomas. 1988. Effects of AMPPNP on the orientation and rotational dynamics of spin-labeled muscle cross-bridges. *Biophys. J.* 53:513–524.

Fajer, P. G., E. A. Fajer, and D. D. Thomas. 1990. Myosin heads have a broad orientational distribution during isometric muscle contraction: time-resolved EPR studies using caged ATP. *Proc. Natl. Acad. Sci. USA.* 87:5538–5542.

Fajer, P. G., E. A. Fajer, M. Schoenberg, D. D. Thomas. 1991. Orientational disorder and motion of weakly attached cross-bridges. *Biophys. J.* 60: 642–649.

Finer, J. T., R. M. Simmons, and J. A. Spudich. 1994. Single myosin molecule mechanics: piconewton forces and nanometre steps. *Nature.* 368: 113–119.

Fryer, M. W., I. R. Neering, and D. G. Stephenson. 1988. Effects of 2,3-butanedione monoxime on the contractile activation properties of fast- and slow-twitch rat muscle contraction. *J. Physiol.* 407:53–75.

Goldman, Y. E. 1987. Kinetics of the actomyosin ATPase in muscle fibers. *Annu. Rev. Physiol.* 49:632–654.

Herrmann, C., J. Wray, F. Travers, and T. Barman. 1992. Effects of 2,3-butanedione monoxime on myosin and myofibrillar ATPase: an example of an uncompetitive inhibitor. *Biochemistry.* 31:12227–12232.

Hibberd, M. G., J. A. Dantzig, D. R. Trentham, and Y. E. Goldman. 1985. Phosphate release and force generation in skeletal muscle fibers. *Science.* 228:1317–1319.

Hibberd, M. G., and D. R. Trentham. 1986. Relationships between chemical and mechanical events during muscular contraction. *Annu. Rev. Biophys. Biophys. Chem.* 15:119–161.

Higuchi, H., and S. Takemori. 1989. Butanedione monoxime suppresses contraction and ATPase activity of rabbit skeletal muscle. *J. Biochem.* 105:638–643.

Homes, K. C., D. Popp, W. Gebhardt, W. Kabsch. 1990. Atomic model of the actin filament. *Nature.* 347:44–49.

Horiuti, K., H. Higuchi, Y. Umazume, M. Konishi, O. Okazaki, and S. Kurihara. 1988. Mechanism of action of 2,3-butanedione 2-monoxime on contraction of frog skeletal muscle fibers. *J. Muscle Res. Cell Motil.* 9:156–164.

Lanzetta, P. A. L. J. Alvarez, D. S. Reinach, and O. A Candia. 1979. Improved assay for nanomole amounts of inorganic phosphate. *Anal. Biochem.* 100:95–97.

Meyer, R. A., H. L. Sweeney, and M. J. Kushmerick. 1984. A simple analysis of the "phosphocreatine shuttle". *Am. J. Physiol.* 246:C365-C377.

Mulieri, L. A., and N. R. Alpert. 1984. Differential effects of 2,3-butanedione monoxime (BDM) on activation and contraction. *Biophys. J.* 45:47a.

Pate, E., and R. Cooke. 1985. The inhibition of muscle contraction by adenosine 5′ (β, γ - imido) triphosphate and by pyrophosphate. *Biophys. J.* 47:773–780.

Pate, E., and R. Cooke. 1988. Energetics of the actomyosin bond in the filament array of muscle fiber. *Biophys. J.* 53:561–573.

Pate, E., L. Nakamaye, K. Franks-Skiba, R. G. Yount, and R. Cooke. 1991. Mechanics of glycerinated muscle fibers using nonnucleoside triphosphate substrates. *Biophys. J.* 59:598–605.

Pate, E., J, Riley, and R. Cooke. 1992. Cross-bridge orientations in muscle fibers activated in GTP, CTP, and ATP. *Biophys. J.* 61:A268.

Pate, E., K. Franks, H. White, and R. Cooke. 1993. The use of differing nucleotides to investigate cross-bridge kinetics. *J. Biol. Chem.* 268: 10046–10053.

Pate, E., G. Wilson, M. Bhimani, and R. Cooke. 1994. The temperature dependence of the inhibitory effects of ortho vanadate on shortening velocity in chemically skinned fast skeletal muscle. *Biophys. J.* 66: 1554–1562.

Raucher, D., and P. G. Fajer. 1994. Orientation and dynamics of myosin heads in aluminum fluoride induced pre-power stroke states: an EPR study. *Biochemistry.* 33:11993–11999.

Rayment, I., H. M. Holden, M. Whittaker, C. B. Yohn, M. Lorenz, K. C. Holmes, and R. A. Milligan. 1993. Structure of the actin-myosin complex and its implications for muscle contraction. *Science.* 261:58–65.

Rayment, I., W. R. Rypniewski, K. Schmidt-Base, R. Smith, D. R. Tomchick, M. M. Benning, D. A. Winkelmann, G. Wesenberg, and H. M. Holden. 1993. A three-dimensional structure of myosin subfragment-1: a molecular motor. *Science.* 261:50–57.

Schroder, R. R., D. J. Manstein, W. John, H. Holden, I. Rayment, K. C. Holmes, and J. A. Spudich. 1993. Three-dimensional atomic model of F-actin decorated with dictyostelium myosin S1. *Nature.* 364:171–174.

Sleep, J. A., K. M. Tryrus, K. A. Johnson, and E. W. Taylor. 1981. Kinetic studies of normal and modified heavy meromyosin and subfragment-1. *J. Muscle Res. Cell Motil.* 2:373–399.

Svensson, E. C., and D. D. Thomas. 1986. ATP induces microsecond rotational motions of myosin heads cross-linked to actin. *Biophys. J.* 50: 999–1002.

Tanner, J. W., D. W. Thomas, and Y. E. Goldman. 1992. Transients in orientation of a fluorescent cross-bridge probe following photolysis of caged nucleotides in skeletal muscle fibers. *J. Mol. Biol.* 223:185–203.

Thomas, D. D. 1987. Spectroscopic probes of muscle cross-bridge rotation. *Annu. Rev. Physiol.* 49:691–709.

Thomas, D. D., and R. Cooke. 1980. Orientation of spin-labeled myosin heads in glycerinated muscle fibers. *Biophys. J.* 32:890–906.

Thomas, D. D., S. Ishiwata, J. C. Seidel, and J. Gergley. 1980. Submillisecond rotational dynamics of spin-labeled cross-bridge in myofibers. *Biophys. J.* 32:873–890.

Thomas, D. D., E. M. Ostap, C. L. Berger, S. M. Lewis, P. G. Fajer, and J. E. Mahaney. 1993. Transient EPR of spin-labeled proteins. *Biol. Mag. Res.* 13:323–351.

Tonomura, Y., P. Apel, and M. F. Morales. 1966. On the molecular weight of myosin. II. *Biochemistry.* 5:515–521.

Wilson, G., S. Shull, and R. Cooke. 1995. Inhibition of muscle force by vanadate. *Biophys. J.* 68:216–226.

Yagi, N., S. Takemori, M. Watanabe, K. Horiuti, and Y. Amemiya. 1992. Effects of 2,3-butanedione monoxime on contraction of frog skeletal muscles: an x-ray diffraction study. *J. Muscle Res. Cell Motil.* 13: 153–106.

Yanagida, T., Kuranaga, and A. Inoue. 1982. Interaction of myosin with filaments during contraction and relaxation: effect of ionic strength. *J. Biochem.* 92:407–412.

Yu, L. C., and V. Brenner. 1989. Structures of actomyosin cross-bridges in relaxed and rigor muscle fibers. *Biophys. J.* 55:441–453.

Zhao, Y., and M. Kawai. 1994. BDM affects nucleotide binding and force generation steps of the cross-bridge cycle in rabbit psoas muscle fibers. *Am. J. Physiol.* 266:C437–447.

Zhao, L., E. Pate, A. J. Baker, and R. Cooke. 1995. Myosin catalytic domain does not rotate during the working powerstroke. *Biophys. J.* In press.